

Interactive tissue reactions of 1064-nm focused picosecond-domain laser and dermal cohesive polydensified matrix hyaluronic acid treatment in in vivo rat skin

Hee Kyung Kim¹ | Hyun-Jo Kim² | Jeong Yeon Hong³ | Jinyoung Park⁴ | Hee Chul Lee⁴ | Herin Lyu⁴ | Sung Bin Cho^{5,6} 

¹Department of Pathology, Soonchunhyang University Bucheon Hospital, Bucheon, Korea

²CNP Skin Clinic, Cheonan, Korea

³Department of Dermatology, Soonchunhyang University College of Medicine, Cheonan, Korea

⁴R&D Center, Lutronic Corporation, Goyang, Korea

⁵Department of Dermatology and Cutaneous Biology Research Center, International St. Mary's Hospital, Catholic Kwandong University College of Medicine, Incheon, Korea

⁶Yonsei Seran Dermatology and Laser Clinic, Seoul, Korea

Correspondence

Sung Bin Cho, Department of Dermatology and Cutaneous Biology Research Center, International St. Mary's Hospital, Catholic Kwandong University College of Medicine, 25 Simgok-ro, Seo-gu, Incheon 22711, Korea.
Email: drsbcho@gmail.com

Abstract

Background: Picosecond-domain laser treatment using a microlens array (MLA) or a diffractive optical element (DOE) generates micro-injury zones in the epidermis and upper dermis.

Objective: To investigate interactive tissue reactions between MLA-type picosecond laser pulses and cohesive polydensified matrix hyaluronic acid (CPMHA) filler in the dermis.

Methods: In vivo rats with or without CPMHA pretreatment were treated with a 1064-nm picosecond-domain neodymium:yttrium-aluminum-garnet (Nd:YAG) laser using an MLA or DOE. Skin samples were obtained at post-treatment days 1, 10, and 21 and histologically and immunohistochemically analyzed.

Results: Picosecond-domain Nd:YAG laser treatment with an MLA-type or a DOE-type handpiece generated fractionated zones of pseudo-cystic cavitation along the lower epidermis and/or upper papillary dermis at Day 1. At Day 21, epidermal thickness, dermal fibroblasts, and collagen fibers had increased. Compared to CPMHA-untreated rats, rats pretreated with CPMHA showed marked increases in fibroblasts and collagen fibers in the papillary dermis. Immunohistochemical staining for the hyaluronic acid receptor CD44 revealed that MLA-type picosecond laser treatment upregulated CD44 expression in the basilar epidermis and dermal fibroblasts.

Conclusions: We suggest that the hyaluronic acid-rich environment associated with CPMHA treatment may enhance MLA-type picosecond-domain laser-induced tissue reactions in the epidermis and upper dermis.

KEYWORDS

CD44, cohesive polydensified matrix hyaluronic acid, laser, laser-induced tissue breakdown, neodymium-doped yttrium aluminum garnet, picosecond

1 | INTRODUCTION

Picosecond-domain laser treatment using a microlens array (MLA) or a diffractive optical element (DOE) has been shown to improve atrophic scars and wrinkles by generating micro-injury zones in the epidermis, basement membrane, and upper dermis.¹⁻⁵ The histologic patterns of vacuolar changes resulting therefrom have been shown to depend on treatment settings, including the melanin index of the target tissue, the wavelength and power density of the picosecond laser, and the distance between the microlens and target tissue.⁶⁻⁸ Whereas the focused picosecond pulses of a 755-nm alexandrite laser generate large vacuoles primarily in the epidermis, those of 532-nm and 1064-nm neodymium:yttrium-aluminum-garnet (Nd:YAG) lasers generate large vacuoles in both the epidermis and the upper dermis. In skin with a higher melanin index, picosecond laser treatment using an MLA or DOE optic generates larger and more vacuoles, and generally, intraepidermal vacuoles are found to be larger than intradermal vacuoles.^{1-2,6-8}

By direct space filling and inducing neocollagenesis, biocompatible, biodegradable, injectable hyaluronic acid (HA) derivatives are indicated for correcting aging-related volume loss and atrophic scars.⁹ HA is a high molecular weight linear polysaccharide naturally present in the extracellular matrix of body tissues, including the epidermis and dermis.⁹⁻¹¹ In addition to its structural properties in the extracellular matrix, HA moisturizes the skin by binding to water and regulates the proliferation and differentiation of various cellular components.^{9,12} The predominant cell surface receptor that mediates the biological functions of HA in the skin is cluster of differentiation 44 (CD44), which acts as a co-receptor for growth factors and cytokine receptors.¹³ In aged skin, the production of HA and the expression of CD44 are downregulated.¹⁴

In this study, we evaluated patterns of picosecond laser-induced micro-injury zones using an MLA or DOE in an in vivo rat model without melanin chromophores in the epidermis. We also investigated interactive tissue reactions between MLA-type picosecond laser pulses and cohesive polydensified matrix hyaluronic acid (CPMHA) filler in the dermis. To do so, rats were treated in vivo with a 1064-nm picosecond-domain Nd:YAG laser using an MLA or DOE with or without CPMHA pretreatment. After treatment, skin samples from the rats were obtained at days 1, 10, and 21, and the patterns of picosecond-induced tissue reactions and interactive tissue reactions between picosecond laser pulses and CPMHA filler were histologically and immunohistochemically evaluated.

2 | METHODS

2.1 | Laser devices

A 1064-nm picosecond-domain Nd:YAG laser device (PicoPlus; Lutronic Corp.) with a pulse duration of 450 picoseconds was used in this study. Using the device, laser energy can be delivered to target tissue as a single flat-top beam, an MLA-type beam, or a DOE-type

beam depending on the desired therapeutic purposes. Using the MLA-type optic array, we emitted a single pulse of picosecond laser energy comprising 113 microbeams at spot size of a 6 mm and a distance between the microlens and the skin of 31 mm. With the DOE-type optic array, we delivered a single pulse of picosecond laser energy comprising 81 microbeams uniformly arranged in a 7 mm × 7 mm square-shaped spot and a 9 × 9 pattern. Furthermore, in addition to a single-pulse mode, a dual-pulse mode, which delivered laser energy through two consecutive, half-fluenced, 450-picosecond pulses at an inter-pulse interval of 1.5 nanoseconds, was also utilized.

2.2 | Pretreatment of in vivo rat skin with CPMHA

All experimental protocols were approved by the ethics committee of the Soonchunhyang University Institutional Animal Care and Use Committee, and all experiments were performed in triplicate. Nine male Sprague-Dawley rats were purchased from Orient Bio at the age of 6 weeks, and the in vivo experiments were performed at the age of 14 weeks at weights of 450-500 g. After gently removing hair on the backs of the rats, the skin was cleansed with 70% alcohol. Then, the skin was marked with black ink to outline grids for each experimental setting (1 cm in diameter/grid; 3-6 grids/rat; a total of 39 grids). Each grid was placed at least 2 cm from the others to minimize the effects of CPMHA and picosecond-domain laser-induced photothermal and photoacoustic effects on adjacent areas.

The CPMHA (BELOTERO BALANCE; Anteis SA) used in this study comprised a total HA concentration of 22.5 mg/mL containing 0.3% lidocaine and was injected subdermally using a 13-mm, 30-gauge needle.¹⁵ The CPMHA was manufactured by fermenting *Streptococcus equi* and processing via two sequential cross-linking steps.¹⁵ Under ether anesthesia, the rat skin was injected with the CPMHA at an angle of needle penetration of 20°-25° to the skin surface with the bevel up while drawing back the needle at a CPMHA volume of 0.1 mL per each grid. Immediately after the injection, any CPMHA-induced lumps were gently massaged and pressed using a cotton-tipped applicator.

2.3 | Picosecond-domain laser treatment

Immediately after subdermal CPMHA infiltration, picosecond Nd:YAG laser treatment was performed on each grid of the in vivo rat skin with or without CPMHA pretreatment. Using an MLA-type handpiece, picosecond Nd:YAG laser treatment at a wavelength of 1064 nm was performed separately on each grid with a spot size of 6 mm, a laser fluence of 1.5 J/cm², a frequency of 5 Hz, and a distance step of 31 mm over two passes (peak power, 3.3 × 10⁹ W/cm²; power density of each microbeam, 3.1 × 10¹⁰ W/cm²). As a control, picosecond laser treatment using a DOE-type handpiece at a wavelength of 1064 nm was delivered to the in vivo rat skin

without CPMHA pretreatment at a spot size of 7 mm and a laser fluence of 0.6 J/cm^2 (peak power, $1.3 \times 10^9 \text{ W/cm}^2$; power density of each microbeam, $1.1 \times 10^{11} \text{ W/cm}^2$) over two passes at 5 Hz using single-pulse and dual-pulse modes. Immediately after picosecond laser treatment with or without CPMHA pretreatment, the treated area was cleansed with 70% alcohol. Neither systemic nor topical corticosteroids and antibiotics were administered prophylactically to the in vivo rats.

2.4 | Histopathological and immunohistochemical studies

Rat tissue samples for each treatment setting were obtained at 1 hour, 10 days, and 21 days after treatment, collecting the epidermis, dermis, and subcutaneous fat. The tissue samples were fixed in 10% buffered formalin and embedded in paraffin. Then, serial tissue sections, which were cut along the longitudinal plane at a thickness of $5 \mu\text{m}$ for each condition, were prepared and stained with hematoxylin and eosin. Additionally, tissue sections from the in vivo rat skin were subjected to immunohistochemical staining for CD44. Briefly, slides were incubated with rabbit anti-CD44 polyclonal antibody (ab157107; Abcam) at a dilution of 1:50. They were further incubated with a secondary antibody (REAL™ EnVision™ HRP Rabbit/Mouse Detection System; Dako) for 30 minutes at room temperature. Then, sections were developed with 3,3'-diaminobenzidine chromogen and counterstained with hematoxylin. Negative controls were obtained by omitting the primary antibody.

3 | RESULTS

3.1 | Picosecond laser-induced rat skin reactions using an MLA or DOE

Immediately after the two passes of picosecond laser treatment using the MLA-type handpiece, well-demarcated pseudo-cystic zones of laser-induced tissue reaction appeared in the epidermis, dermoepidermal junction, and upper papillary dermis (Figure 1A). The histologic features of thermal tissue coagulation were occasionally found within or around the pseudo-cystic zones. At Day 21, the laser-treated skin had completely repaired, with notable increases in epidermal thickness and in fibroblasts and collagen fibers in the upper papillary dermis, compared with untreated control rat skin (Figure 1B).

Immediately after the two passes of picosecond laser treatment using the DOE-type handpiece in the single-pulse mode, well-demarcated pseudo-cystic zones were found in the upper dermis with or without laser-induced tissue reactions in the epidermis and dermoepidermal junction (Figure 1C). Using the DOE, histologic features of thermal tissue coagulation were less remarkable than those generated with the MLA optic, although extravasation of

red blood cells within or around the pseudo-cystic zones was more extensive. Meanwhile, treatment in the dual-pulse mode generated greater pseudo-cystic tissue reactions in the upper dermis without remarkable extravasation of red blood cells (Figure 1D). At Day 21, skin specimens exhibited increases in epidermal thickness and in fibroblasts and collagen fibers in the upper dermis (data not shown).

3.2 | Picosecond laser-induced tissue reactions in in vivo rat skin with CPMHA pretreatment

At Day 1, rat skin pretreated with CPMHA showed extensive infiltration of CPMHA into the deep dermis, subcutaneous fat, and fascia layers (Figure 2A, B). Moreover, CPMHA had infiltrated through collagen bundles in the upper dermis and mid-dermis (Figure 2C). After picosecond laser treatment, pseudo-cystic zones were found in the epidermis, dermoepidermal junction, and upper dermis (Figure 2D). No remarkable histologic features suggestive of picosecond laser-induced CPMHA destruction were found in any layer of the rat skin.

At Day 10, CPMHA was more homogeneously distributed throughout the deep dermis, subcutaneous fat, and fascia layers, compared with Day 1 (Figure 3A, B). Moreover, CPMHA in the upper dermis and mid-dermis had been infiltrated with numerous dermal fibroblasts (Figure 3C). Picosecond laser-induced pseudo-cystic tissue reactions had disappeared, and the epidermis was markedly thickened (Figure 3D). The upper dermis showed marked infiltration of fibroblasts and inflammatory cells, along with dilated microvascular components.

At Day 21, the area of CPMHA infiltration had decreased, although the histologic patterns thereof were more homogenous and obvious in the deep dermis, subcutaneous fat, and fascia layers, compared with Day 1 and Day 10 (Figure 4A-C). Infiltration of CPMHA was also found in the mid-dermis, but not in the upper papillary dermis (Figure 4C). Fibroblast and collagen fiber amounts were greater in the dermis in laser-treated skin pretreated with CPMHA, compared with untreated control and MLA-treated, CPMHA-untreated rat skin (Figure 4D).

3.3 | Picosecond laser-induced CD44 expression in HA-rich rat skin

Untreated control rat skin showed immunoreactivity for CD44 in the cytoplasm of epidermal keratinocytes and upper dermal fibroblasts (Figure 5A). However, the CD44 immunoreactivity of mesenchymal cells in the deep dermis, subcutaneous fat, and fascia layers was unremarkable (Figure 5B). At Day 1 after laser treatment, rat skin pretreated with CPMHA exhibited marked upregulation of CD44 expression in the cytoplasm of basilar keratinocytes around the laser-induced pseudo-cystic areas (Figure 5C). Dermal fibroblasts presented similar CD44 immunoreactivity, compared with untreated rat skin. Moreover, CD44 immunoreactivity of mesenchymal cells

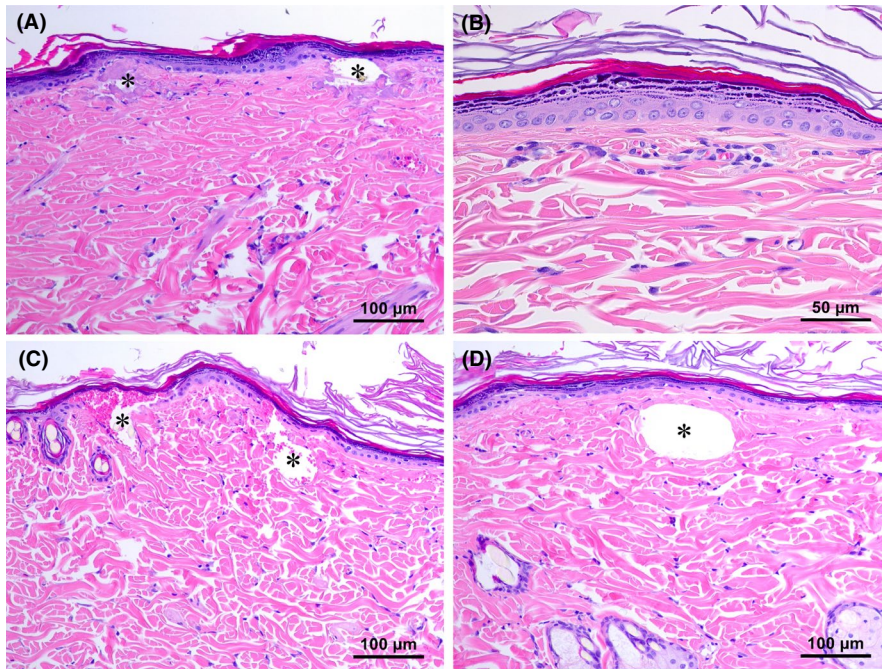


FIGURE 1 Picosecond laser-induced rat skin reactions. Immediately after picosecond laser treatment using a microlens array (MLA)-type handpiece (A) and 21 days post-treatment (B). Immediately after laser treatment using a diffractive optical element-type handpiece in a single-pulse mode (C) and a dual-pulse mode (D). Asterisks indicate pseudo-cystic zones of laser-induced tissue reaction. H&E stain at original magnification $\times 200$ (A, C, D) and $\times 400$ (B). Scale bar = 100 μm (A, C, D) and 50 μm (B)

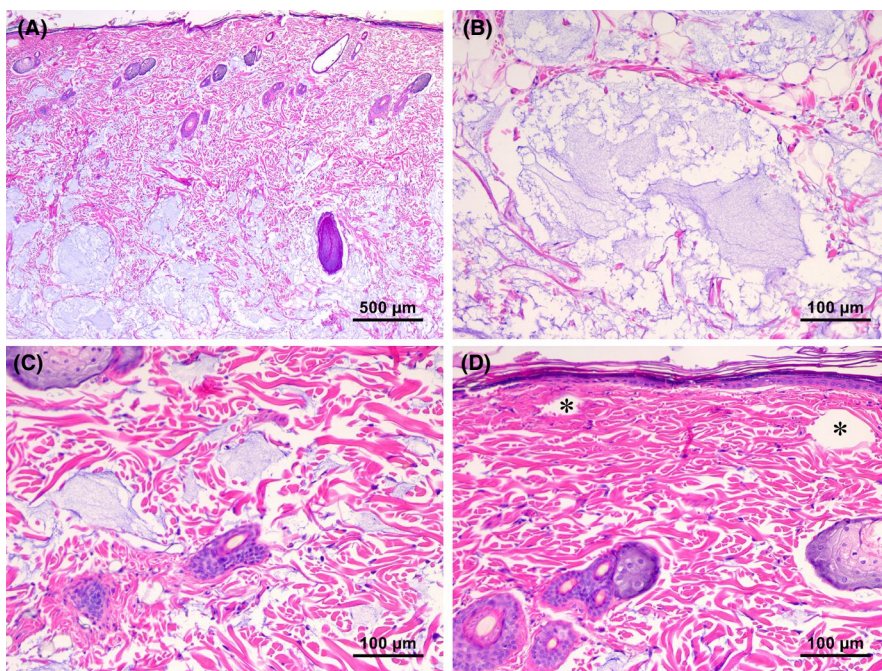


FIGURE 2 Immediate picosecond laser-induced tissue reactions in in vivo rat skin pretreated with cohesive polydensified matrix hyaluronic acid (CPMHA). Immediately after picosecond laser treatment using an microlens array (MLA)-type handpiece in CPMHA-pretreated in vivo rat skin (A). CPMHA infiltrated the deep dermis and subcutaneous fat layers (B) and the mid-dermis (C). Pseudo-cystic zones of laser-induced tissue reactions (asterisks) and CPMHA infiltration in the upper dermis (D). H&E stain at original magnification $\times 40$ (A) and $\times 200$ (B-D). Scale bar = 500 μm (A) and 100 μm (B-D)

was unremarkable in the deep dermis, subcutaneous fat, and fascia layers of skin showing extensive infiltration of CPMHA (Figure 5D).

At Day 10 after laser treatment, upregulated CD44 immunoreactivity was found in basilar keratinocytes, although the intensity thereof was lower than that at Day 1 (Figure 6A). Dermal fibroblasts and mesenchymal cells in the deep dermis, subcutaneous fat, and fascia layers presented similar patterns of CD44 expression as those in untreated rat skin and Day 1 rat skin (Figure 6B). At Day 21, increased CD44 immunoreactivity was still observed in basilar keratinocytes, although at an intensity lower than that at Day 1 and Day 10 (Figure 6C). Rat skin at Day 21 presents marked increases

in fibroblasts and collagen fibers in the upper dermis, but negative immunoreactivity for CD44. The CD44 immunoreactivity of mesenchymal cells in the CPMHA-infiltrated deep dermis, subcutaneous fat, and fascia layers was also unremarkable (Figure 6D).

4 | DISCUSSION

Picosecond laser-induced micro-injury zones present histologically as a few large, pseudo-cystic vacuoles and/or numerous perinuclear microscopic vacuoles in the epidermis and upper dermis.^{2,6-8} The

FIGURE 3 Picosecond laser-induced tissue reactions after 10 days in in vivo rat skin pretreated with cohesive polydensified matrix hyaluronic acid (CPMHA). Rat skin pretreated with CPMHA at 10 days after MLA-type laser treatment (A). Infiltration of CPMHA in the deep dermis and subcutaneous fat layers (B) and in the mid-dermis (C). CPMHA infiltration in the upper dermis and thickening of the epidermis, with increased fibroblasts and inflammatory cells (D). H&E stain at original magnification $\times 25$ (A), $\times 200$ (B, C), and $\times 400$ (D). Scale bar = 1 mm (A), 100 μm (B, C), and 50 μm (D)

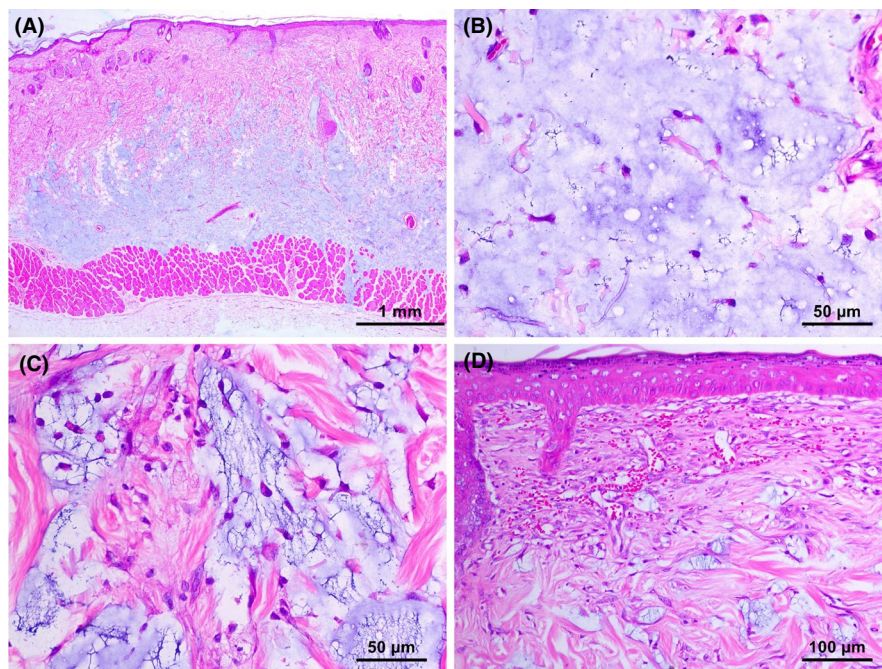
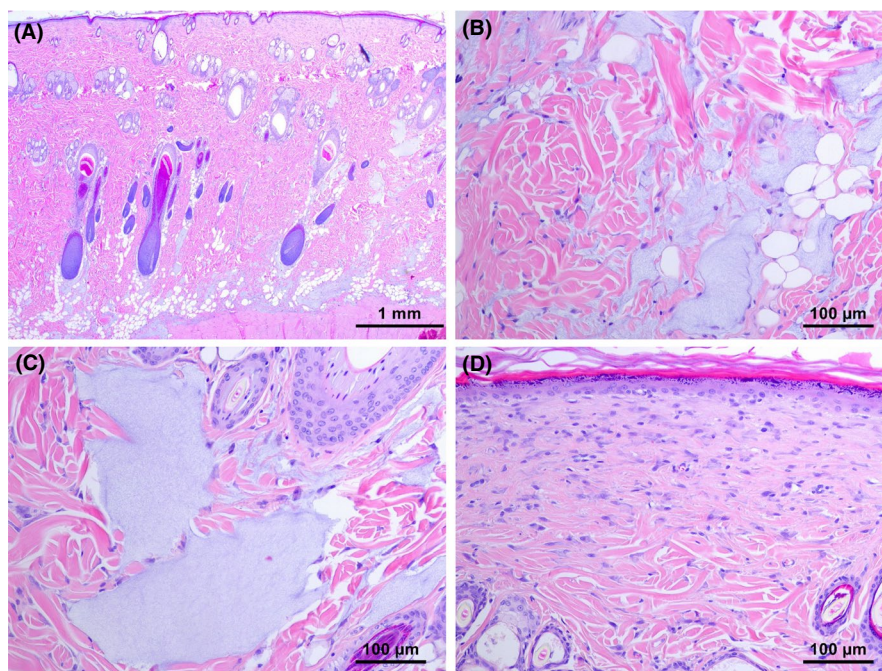


FIGURE 4 Picosecond laser-induced tissue reactions after 21 days in in vivo rat skin pretreated with cohesive polydensified matrix hyaluronic acid (CPMHA). Rat skin pretreated with CPMHA at 21 days after microlens array (MLA)-type laser treatment (A). Infiltration of CPMHA in the deep dermis and subcutaneous fat layers (B) and in the mid-dermis (C). Thickening of the epidermis, with marked increases in fibroblasts and collagen fibers (D). H&E stain at original magnification $\times 25$ (A) and $\times 200$ (B-D). Scale bar = 1 mm (A) and 100 μm (B-D)



generation of micro-injury zones is initiated as the laser stimulates the production of free electrons via multiphoton absorption or thermionic emission, depending on the power density of the picosecond laser pulse and the absorption properties of chromophores in the target tissue.⁵ Theoretically, multiphoton absorption occurs in a chromophore-independent manner at a higher irradiation threshold ($\sim 10^{13} \text{ W/cm}^2$ in water) than thermionic emission, which occurs in a chromophore-dependent manner at a relatively lower irradiation threshold.⁵

Although two passes of picosecond laser treatment at each experimental setting were delivered at 200-msec intervals, the power

density levels of picosecond laser treatments in our study were below the theoretical irradiation threshold for generating free seed electrons via multiphoton absorption.⁵ In our study, we used power density settings for each microbeam of $3.1 \times 10^{10} \text{ W/cm}^2$ when using the MLA-type handpiece and $1.1 \times 10^{11} \text{ W/cm}^2$ when using the DOE-type handpiece. Additionally, picosecond laser treatment in the dual-pulse mode delivered laser energy through two consecutive, 450-psec pulses with a power density of $5.5 \times 10^{10} \text{ W/cm}^2/\text{microbeam}$ at a 1.5-nsec inter-pulse interval. Moreover, rats in the in vivo rat model lacked melanin chromophores in their skin. Nonetheless, large pseudo-cystic vacuoles, rather than microscopic perinuclear vacuoles, were readily

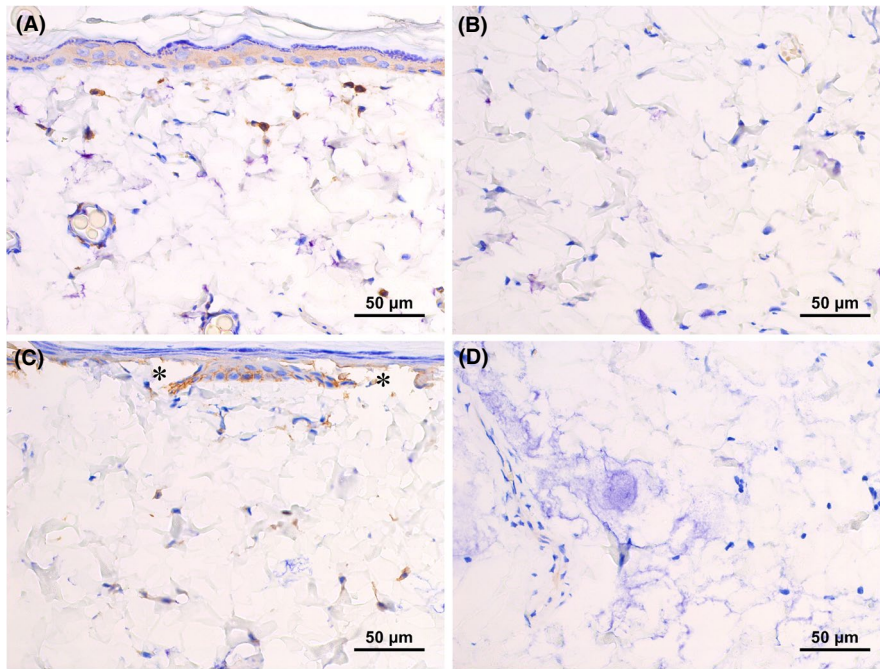


FIGURE 5 CD44 immunoreactivity in picosecond laser-treated in vivo rat skin pretreated with cohesive polydensified matrix hyaluronic acid (CPMHA) immediately after treatment. Untreated control rat skin shows CD44-positive dermal fibroblasts (A) and CD44-negative mesenchymal cells in the deep dermis and subcutaneous fat layers (B). Immediately after picosecond laser treatment using an MLA-type handpiece in CPMHA-pretreated in vivo rat skin (C, D). CD44-positive basilar keratinocytes and dermal fibroblasts (C) and CD44-negative mesenchymal cells in the CPMHA-infiltrated deep dermis and subcutaneous fat layers (D). CD44 immunohistochemical stain at original magnification $\times 400$. Scale bar = 50 μm

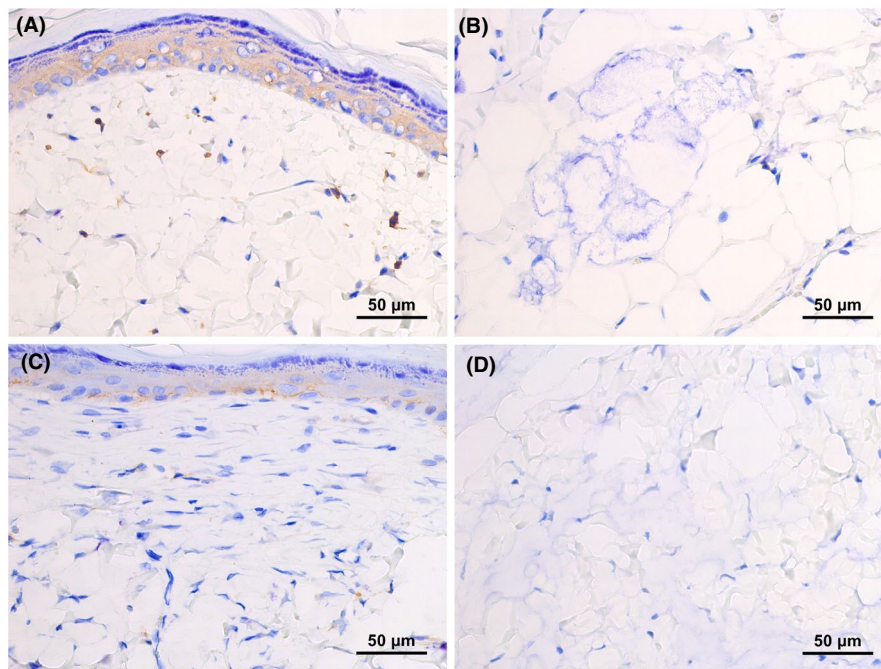


FIGURE 6 CD44 immunoreactivity in picosecond laser-treated in vivo rat skin pretreated with cohesive polydensified matrix hyaluronic acid (CPMHA) at 10 and 21 days after treatment. Ten days post- microlens array (MLA)-type laser treatment on CPMHA-pretreated rat skin (A, B). CD44-positive basilar keratinocytes and dermal fibroblasts (A) and CD44-negative mesenchymal cells in the CPMHA-infiltrated deep dermis and subcutaneous fat layers (B). Twenty-one days post-MLA-type laser treatment on CPMHA-pretreated rat skin (C, D). CD44-positive basilar keratinocytes (C) and CD44-negative fibroblasts in the upper dermis and mesenchymal cells in the CPMHA-infiltrated deep dermis and subcutaneous fat layers (D). CD44 immunohistochemical stain at original magnification $\times 400$. Scale bar = 50 μm

apparent in the lower epidermis, basement membrane, or upper dermis of the in vivo rat skin at Day 1 after laser treatment. Accordingly, we suggest that picosecond laser treatment in in vivo rat skin using an MLA-type handpiece can elicit chromophore-independent tissue reactions of laser-induced optical breakdown at a lower irradiation

threshold via multiphoton absorption, as well as non-melanin chromophore-dependent tissue reactions of laser-induced thermal breakdown via thermionic emission.

In the present study, immunohistochemical staining for CD44 in the rat skin revealed the upregulation of CD44 expression in the

basilar epidermis and dermal fibroblasts upon MLA-type picosecond laser treatment. CD44 is a ubiquitous and functionally important cell surface receptor to which HA binds in the epidermis and dermis to regulate epidermal functions.¹⁶ HA-CD44 interactions have been shown to accelerate wound repair and permeability barrier recovery by upregulating downstream signal pathways, particularly RhoA-Rho-binding kinase and Rac protein kinase N γ pathways, which initiate the onset of multiple cellular functions, including cell-cell adhesion, proliferation, survival, migration, differentiation, and barrier formation.^{16,17}

During wound repair, fibroblasts are the primary source of reparative matrix, and activation and proliferation of resident fibroblasts are considered to be an important early step therein.¹⁸ Transforming growth factor- β 1 (TGF- β 1), in particular, plays an important role in regulating dermal fibrosis, and TGF- β 1-dependent proliferative responses are regulated by HA through CD44.¹⁸ In a HA-rich environment, coupling between epidermal growth factor receptor (EGFR) and CD44 is increased to enhance signal transduction through the mitogen-activated protein kinase (MAPK)/extracellular signal-regulated kinase (ERK) pathway.¹⁸ Thereby, HA promotes EGFR-CD44 interactions and subsequent MAPK/ERK activation that results in TGF- β 1-dependent fibroblast proliferation.¹⁸ Accordingly, through this study, we deemed that the induction of CD44 expression by picosecond laser pulses and enhanced CD44-HA interactions by CPMHA pretreatment may have resulted in the observed stimulation of collagen production in the upper dermis.

In conclusion, our in vivo rat study demonstrated that 1064-nm picosecond-domain Nd:YAG laser treatment using an MLA-type or a DOE-type handpiece generates fractionated zones of pseudo-cystic cavitation along the lower epidermis and/or upper papillary dermis apparent at Day 1 after treatment. At Day 21, epidermal thickness, dermal fibroblasts, and collagen fibers had increased. Picosecond laser treatment of rat skin pretreated with CPMHA, which infiltrated the mid-dermis to deep dermis, was not affected by the picosecond laser pulses. Moreover, fibroblast and collagen fiber amounts in the papillary dermis were markedly greater in the CPMHA-pretreated rat skin than in CPMHA-untreated rat skin. Immunohistochemical staining for the HA receptor CD44 revealed that the MLA-type picosecond laser treatment upregulated CD44 expression in the basilar epidermis and dermal fibroblasts. Although further in vivo human skin study is needed to confirm our findings, we suggest that the HA-rich environment generated by CPMHA pretreatment may enhance MLA-type picosecond-domain laser-induced tissue reactions in the epidermis and upper dermis.

ACKNOWLEDGMENTS

We would like to thank Anthony Thomas Milliken, ELS (Editing Synthese, Seoul, Korea), for his help with the editing of this manuscript.

CONFLICT OF INTEREST

The authors declare no conflicts of interest.

ORCID

Sung Bin Cho  <https://orcid.org/0000-0001-6748-5071>

REFERENCES

1. Balu M, Lentsch G, Korta DZ, et al. In vivo multiphoton-microscopy of picosecond-laser-induced optical breakdown in human skin. *Lasers Surg Med.* 2017;49:555-562.
2. Tanghetti EA. The histology of skin treated with a picosecond alexandrite laser and a fractional lens array. *Lasers Surg Med.* 2016;48:646-652.
3. Brauer JA, Kazlouskaya V, Alabdulrazzaq H, et al. Use of a picosecond pulse duration laser with specialized optic for treatment of facial acne scarring. *JAMA Dermatol.* 2015;151:278-284.
4. Bernstein EF, Schomacker KT, Basilavacchio LD, Plugis JM, Bhawalkar JD. Treatment of acne scarring with a novel fractionated, dual-wavelength, picosecond-domain laser incorporating a novel holographic beam-splitter. *Lasers Surg Med.* 2017;49:796-802.
5. Varghese B, Bonito V, Jurna M, Palero J, Verhagen MH. Influence of absorption induced thermal initiation pathway on irradiance threshold for laser induced breakdown. *Biomed Opt Express.* 2015;6:1234-1240.
6. Tanghetti E, Jennings J. A comparative study with a 755 nm picosecond Alexandrite laser with a diffractive lens array and a 532 nm/1064 nm Nd:YAG with a holographic optic. *Lasers Surg Med.* 2018;50:37-44.
7. Lee HC, Childs J, Chung HJ, Park J, Hong J, Cho SB. Pattern analysis of 532- and 1,064-nm picosecond-domain laser-induced immediate tissue reactions in ex vivo pigmented micropig skin. *Sci Rep.* 2019;9:4186.
8. Chung HJ, Lee HC, Park J, et al. Pattern analysis of 532- and 1064-nm microlens array-type, picosecond-domain laser-induced tissue reactions in ex vivo human skin. *Lasers Med Sci.* 2019;34:1207-1215.
9. Alam M, Tung R. Injection technique in neurotoxins and fillers: indications, products, and outcomes. *J Am Acad Dermatol.* 2018;79:423-435.
10. Tammi R, Ripellino JA, Margolis RU, Tammi M. Localization of epidermal hyaluronic acid using the hyaluronate binding region of cartilage proteoglycan as a specific probe. *J Invest Dermatol.* 1988;90:412-414.
11. Tammi R, MacCallum D, Hascall VC, Pienimäki JP, Hyttinen M, Tammi M. Hyaluronan bound to CD44 on keratinocytes is displaced by hyaluronan decasaccharides and not hexasaccharides. *J Biol Chem.* 1998;273:28878-28888.
12. Lee DH, Oh JH, Chung JH. Glycosaminoglycan and proteoglycan in skin aging. *J Dermatol Sci.* 2016;83:174-181.
13. Underhill C. CD44: the hyaluronan receptor. *J Cell Sci.* 1992;103:293-298.
14. Oh JH, Kim YK, Jung JY, Shin JE, Chung JH. Changes in glycosaminoglycans and related proteoglycans in intrinsically aged human skin in vivo. *Exp Dermatol.* 2011;20:454-456.
15. Sundaram H, Fagien S. Cohesive polydensified matrix hyaluronic acid for fine lines. *Plast Reconstr Surg.* 2015;136:1495-163S.
16. Bourguignon LY. Matrix hyaluronan-activated CD44 signaling promotes keratinocyte activities and improves abnormal epidermal functions. *Am J Pathol.* 2014;184:1912-1919.
17. Turley EA, Nobel PW, Bourguignon LY. Signaling properties of hyaluronan receptors. *J Biol Chem.* 2002;277:4589-4592.
18. Meran S, Luo DD, Simpson R, et al. Hyaluronan facilitates transforming growth factor- β 1-dependent proliferation via CD44 and epidermal growth factor receptor interaction. *J Biol Chem.* 2011;286:17618-17630.

How to cite this article: Kim HK, Kim H-J, Hong JY, et al. Interactive tissue reactions of 1064-nm focused picosecond-domain laser and dermal cohesive polydensified matrix hyaluronic acid treatment in in vivo rat skin. *Skin Res Technol.* 2020;00:1-7. <https://doi.org/10.1111/srt.12853>